

# Dark Matter–Dark Energy coupling biasing parameter estimates from CMB data

Giuseppe La Vacca<sup>1</sup>

*Theoretical and Nuclear Physics Department, Pavia University, Via A. Bassi 6, 20100 Pavia, Italy*

giuseppe.lavacca@mib.infn.it

Loris P.L. Colombo<sup>2</sup>

*Department of Physics & Astronomy, University of Southern California, Los Angeles, CA 90089-0484*

colombo@usc.edu

Luca Vergani

*Physics Dep. G. Occhialini, Milano–Bicocca University, Piazza della Scienza 3, 20126 Milano, Italy*

luca.vergani@mib.infn.it

and

Silvio A. Bonometto<sup>1</sup>

*Physics Dep. G. Occhialini, Milano–Bicocca University, Piazza della Scienza 3, 20126 Milano, Italy*

silvio.bonometto@mib.infn.it

## ABSTRACT

When CMB data are used to derive cosmological parameters, their very choice does matter: some parameter values can be biased if the parameter space does not cover the “true” model. This is a problem, because of the difficulty to

---

<sup>1</sup>I.N.F.N., sez. Milano–Bicocca, Piazza della Scienza 3, 20126 Milano, Italy

<sup>1</sup>Physics Dep. G. Occhialini, Milano–Bicocca University, Piazza della Scienza 3, 20126 Milano, Italy

parametrize Dark Energy (DE) physics. We test this risk through numerical experiments. We create artificial data for dynamical or coupled DE models and then use MCMC techniques to recover model parameters, by assuming a constant DE state parameter  $w$  and no DM–DE coupling. For the DE potential considered, no serious bias arises when coupling is absent. On the contrary,  $\omega_{o,c}$ , and thence  $H_o$  and  $\Omega_{o,m}$ , suffer a serious bias when the “true” cosmology includes even just a mild DM–DE coupling. Until the dark components keep an unknown nature, therefore, it can be important to allow for a degree of freedom accounting for DM–DE coupling, even more than increasing the number of parameters accounting for the  $w(a)$  behavior.

*Subject headings:* Dark Matter – Dark Energy – Cosmic Microwave Background – Cosmological Parameters

## 1. Introduction

Scarce doubts remain that Dark Energy (DE) exists. Not only SNIa data indicate an accelerated cosmic expansion (Perlmutter et al. 1997, 1998, Riess et al. 1998, Foley et al. 2007); also CMB and deep sample data show a clear discrepancy between the total density parameter  $\Omega_o$ , approaching unity, and the matter density parameter  $\Omega_{o,m} \sim 0.25\text{--}0.3$  (see, *e.g.*, Spergel et al. 2007). DE covers this gap; its state parameter  $w \equiv p_{de}/\rho_{de}$  must approach  $-1$  today, so apparently excluding that DE is made of free particles ( $p_{o,de}$ ,  $\rho_{o,de}$ : DE pressure, energy density). The true nature of DE is however still elusive; a false vacuum and a self-interacting scalar field are among the most popular hypotheses for it (Wetterich 1988, Ratra & Peebles 1988).

In this paper we explore some possible consequences of our poor knowledge of DE nature. In particular we test the risk that other cosmological parameter estimates are biased by a inadequate parametrization of the DE component. We shall see that this risk is real.

Theoretical predictions had an astonishing success in fitting CMB data. For instance, the SW effect, predicting low- $l$   $C_l$  data, or primeval compression waves, predicting  $C_l$  peaks and deeps, were clearly detected. There is little doubt that we are exploring the right range of models.

When we investigate DE nature through CMB data, we must bear in mind that they were mostly fixed at a redshift  $z \sim 1100$ , when the very DE density should be negligible, and so affects peak and deep positions indirectly, through the values of  $\omega_{o,c} \equiv \Omega_{o,c}h^2$  and  $\omega_{o,b} \equiv \Omega_{o,b}h^2$  (here  $H_o = 100 h \text{ km/s/Mpc}$  is the present Hubble parameter;  $\Omega_o$ ,  $\Omega_{o,c}$ ,  $\Omega_{o,b}$

are the present total, CDM, baryon density parameters). Later information on DE state equation, conveyed by the ISW effect, is seriously affected by cosmic variance and often relies on the assumption that a single opacity parameter  $\tau$  can account for reionization, assumed to be (almost) instantaneous. Accordingly, if we assume dynamical DE (DDE), due to a scalar field  $\phi$  self interacting through a potential  $V(\phi)$ , CMB data allow to exclude some interaction shape, *e.g.* Ratra–Peebles (1988) potentials with significantly large  $\Lambda$  energy scales, but hardly convey much information on potential parameters.

In spite of that, when we choose a DE potential or a specific scale dependence of the DE state parameter  $w(a)$ , we risk to bias the values of other cosmological parameters, sometimes leading to premature physical conclusions. An example is the value of the primeval spectral index for scalar fluctuation  $n_s$ . Using WMAP3 data (Spergel et al. 2007) and assuming a  $\Lambda$ CDM cosmology, the value  $n_s = 1$  is “excluded” at the  $2\text{-}\sigma$  confidence level. On the contrary, Colombo & Gervasi (2007) showed that this is no longer true in a DDE model based on a SUGRA potential (Brax & Martin 1999, 2001; Brax, Martin & Riazuelo 2000), whose likelihood was the same of  $\Lambda$ CDM.

The risk that our poor knowledge of DE nature biases parameter determination is even more serious if DM–DE coupling is allowed. Coupled DE (CDE) cosmologies were studied by various authors (see, *e.g.*, Wetterich 1995, Amendola 2000, Bento, Bertolami & Sen 2002, Macciò et al. 2004).

While DDE was introduced in the attempt to ease DE *fine-tuning* problems, CDE tries to ease the *coincidence* problem. Let us then parametrise the strength of DM–DE coupling through a parameter  $\beta$ , defined below. When  $\beta$  is large enough, DM and DE scale (quasi) in parallel since a fairly high redshift. In turn this modifies the rate of cosmic expansion whenever DM and/or DE contributions to the total energy density are non-negligible, so that limits on  $\beta$  can be set through data.

The range allowed ( $\beta < 0.10\text{--}0.12$ ; Mainini, Colombo & Bonometto 2005, Mainini & Bonometto 2007, see also Majerotto, Sapone & Amendola 2004, Amendola, Campos & Rosenfeld, 2006), unfortunately, is so limited that DM and DE are doomed to scale differently, but in a short redshift interval. Clearly, this spoils the initial motivation of coupling, but, once the genie is outside the lamp, it is hard to put him back inside: even though the coupling solves little conceptual problems, we should verify that no bias arises on the other parameters, for the neglect of  $\beta$ ’s consistent with data. This is far from being just a theoretical loophole, the still unknown physics of the dark components could really imply the presence of a mild DM–DE coupling, and its discovery could mark a step forwards in the understanding of their nature.

Here we test this possibility by performing some numerical experiments. We assume DDE and CDE due to a SUGRA potential and use MCMC techniques to fit the following parameter set:  $\omega_{o,c}$ ,  $\omega_{o,b}$ ,  $\tau$ ,  $\theta$ ,  $n_s$ ,  $A_s$  and (constant)  $w$ ;  $\theta$  is the angular size of the sound horizon at recombination (see however below),  $n_s$  and  $A_s$  are spectral index and amplitude of scalar waves, no tensor mode is considered.

The plan of the paper is as follows: In Section 2 we discuss how artificial data are built, outlining the models selected, the DDE potential used and the sensitivity assumed. In Section 3 we briefly debate the features of the MCMC algorithm used and illustrate a test on its efficiency, also outlining the physical reasons why some variables are more or less efficiently recovered. In Section 4 we discuss the results of an analysis of DDE artificial data, against the  $w = \text{const.}$  assumption. In Section 5 we briefly summarize why and how CDE models are built and do the same of Sec. 4 for CDE models. This section yields the most significant results of this work. In Section 6 we draw our conclusions.

## 2. Building artificial data

In order to produce artificial data we use CAMB, or a suitable extension of it (see below), to derive the angular spectra  $C_l^{(TT)}$ ,  $C_l^{(EE)}$ ,  $C_l^{(TE)}$  for various sets of parameter values. Artificial data are then worked out from spectra, according to Perotto et al. (2006).

The analysis we report is however mostly based on a single choice of parameters, WMAP5 inspired (see Komatsu et al., 2008, Spergel et al. 2007), in association with three different  $\beta$ 's. Two other parameter choices will also be used: (i) to test the efficiency of the MCMC algorithm; (ii) to add results for a still lower  $\beta$  value, so strengthening our conclusions.

The parameter sets for the most general case and the (ii) case are shown in Table 1. In these cases DE is due to a scalar field self-interacting through a SUGRA potential

$$V(\phi) = (\Lambda^{\alpha+4}/\phi^\alpha) \exp(4\pi \phi^2/m_p^2) , \quad (1)$$

( $m_p$  : Planck mass) which has been shown to fit CMB data at least as well as  $\Lambda$ CDM (Colombo & Gervasi 2007); as outlined in the Table, we input the value of the energy scale  $\Lambda$ ; the corresponding  $\alpha$  value is determined by the program itself; the choice  $\Lambda = 1 \text{ GeV}$  is consistent with Colombo & Gervasi (2007) findings and is however scarcely constrained by data. The meaning of the coupling constant  $\beta$  is discussed at the beginning of Section 5.

Starting from the spectral components and assuming that cosmic fluctuations are distributed according to a Gaussian process, we generate *realizations* of the coefficients of the

	Model A	Model B
$\Omega_o$	1	1
$10^2 \omega_{o,b}$	2.273	2.4
$\omega_{o,c}$	0.1099	0.11
$100 h$	71.9	85
$\tau_{opt}$	0.087	0.15
$\ln(10^{10} A_s)$	3.1634	3.1355
$n_s$	0.963	1
$\Lambda/\text{GeV}$	1	1
	0	
$\beta$	0.05	0.02
	0.10	

Table 1: *Cosmological parameters for artificial CMB data.*

spherical harmonic expansions for the temperature and E-polarization fields, according to the expressions

$$a_{lm}^{(T)} = \sqrt{C_l^{(TT)}} g_{lm}^{(1)} , \quad (2)$$

$$a_{lm}^{(E)} = \left[ C_l^{(TE)} / C_l^{(TT)} \right] \sqrt{C_l^{(TT)}} g_{lm}^{(1)} + \sqrt{C_l^{(EE)} - \left[ \left( C_l^{(TE)} \right)^2 / C_l^{(TT)} \right]} g_{lm}^{(2)} , \quad (3)$$

where both  $g_{lm}^{(i)}$ , for any  $l$  and  $m$ , are casual variables, distributed in a Gaussian way with null averages and unit variance, so that the equality  $\langle g_{lm}^{(i)} g_{lm}^{(j)} \rangle = \delta^{ij}$  is approached when the number of realizations increases. Together with eqs. (2) and (3) this grants that

$$\begin{aligned} \langle a_{lm}^{(T)} a_{l'm'}^{(T)*} \rangle &= C_l^{(TT)} \delta_{ll'} \delta_{mm'} , & \langle a_{lm}^{(E)} a_{l'm'}^{(E)*} \rangle &= C_l^{(EE)} \delta_{ll'} \delta_{mm'} , \\ \langle a_{lm}^{(T)} a_{l'm'}^{(E)*} \rangle &= C_l^{(TE)} \delta_{ll'} \delta_{mm'} , \end{aligned} \quad (4)$$

if averages are taken over an “infinite” set of sky realizations. From a single realization, we can define estimators of the power as

$$\begin{aligned} (2l+1) \hat{C}_l^{(TT)} &= \sum_m a_{lm}^{(T)} a_{lm}^{(T)*} , & (2l+1) \hat{C}_l^{(EE)} &= \sum_m a_{lm}^{(E)} a_{lm}^{(E)*} , \\ (2l+1) \hat{C}_l^{(TE)} &= \sum_m a_{lm}^{(T)} a_{lm}^{(E)*} . \end{aligned} \quad (5)$$

Taken independently from each other,  $\hat{C}_l^{(TT)}$  and  $\hat{C}_l^{(EE)}$  at a given  $l$  are the sum of the squares of  $2l+1$  Gaussian random variables, so they are distributed according to a  $\chi^2$  with  $2l+1$ , which approaches a Gaussian distribution centered around the fiducial  $C_l^{(TT)}$ ,  $C_l^{(EE)}$ , values,

as  $l$  increases. If we consider  $T$  and  $E$  simultaneously, the set of estimators  $\hat{C}_l^{(TT)}$ ,  $\hat{C}_l^{(EE)}$ ,  $\hat{C}_l^{(TE)}$  follow a Wishart distribution (see, e.g., Percival & Brown 2006).

We consider here an idealized full-sky experiment characterized by: (i) finite resolution, that we shall set through a Full Width Half Maximum angle  $\vartheta_{FWHM}$ , where the antenna sensitivity is reduced to 50 %, assuming a circularly symmetric Gaussian beam profile; (ii) background noise due to the apparatus, that we shall assume to be *white*, i.e.  $l$ -independent with an assigned variance  $\sigma_N^2$ .

More in detail: for what concerns the Gaussian and circularly symmetric beam profile, its window function reads

$${}_s B_l = e^{-[l(l+1)-s^2]\sigma^2/2} , \quad \text{with} \quad \sigma \equiv \vartheta_{FWHM}/\sqrt{8 \ln 2} , \quad (6)$$

$s$  being the spin of the signal (0 for anisotropy or  $E$ -polarization spectra; its value however matters just for the lowest  $l$ 's). For what concerns noise, we shall consider the coefficients  $n_{lm}$  such that

$$\langle a_{lm}^{(R)} n_{l'm'}^{(S)*} \rangle = 0 , \quad \langle n_{lm}^{(R)} n_{l'm'}^{(S)*} \rangle = N_l^{(RS)} \delta_{ll'} \delta_{mm'} , \quad (7)$$

with  $N_l^{(RS)} = \sigma_N^2 \delta^{RS}$ , and  $R$  and  $S$  stand for either  $T$  or  $E$ . As the sum of two independent Gaussian random variables is still Gaussian distributed, the statistics of the (beam-convolved) CMB +white noise field are given by  $\mathcal{C}_l^{(RS)} = C_l^{(RS)} |{}_0 B_l|^2 + N_l^{(RS)}$ . In an analogous manner from  $\hat{C}_l^{(RS)}$  we can define  $\hat{\mathcal{C}}_l^{(RS)}$ . In the following we will consider both *fiducial*, i.e.  $\mathcal{C}_l^{(RS)}$ , or *realized*,  $\hat{\mathcal{C}}_l^{(RS)}$ , model data sets.

Under these simplified assumptions, the characteristics of an experiment are completely defined by the values of  $\vartheta_{FWHM}$  and  $\sigma_N^2$ . Here we shall take  $\vartheta_{FWHM} \simeq 7.0'$ , while  $\sigma_T^2 \simeq 3 \times 10^{-4} (\mu\text{K})^2$  and  $\sigma_P^2 \simeq 6 \times 10^{-4} (\mu\text{K})^2$ . These can be considered conservative estimates of sensitivity in the forthcoming Planck experiment.

### 3. The MCMC algorithm

When the number  $\mathcal{N}$  of the parameters to be determined from a given data set is large, the whole  $\mathcal{N}$ -dimensional parameter space cannot be fully explored within a reasonable computing time. MonteCarlo Markov Chain (MCMC) algorithms are then used, whose efficiency and reliability have been widely tested.

In this work we used the MCMC engine and statistical tools provided by the CosmoMC package (Lewis & Bridle 2002; <http://cosmologist.info/cosmomc>). This tool set allows us to work out a suitable set of  $M$  Markov Chains and analyze their statistical properties, both in the full  $\mathcal{N}$ -dimensional parameter space, and in lower dimensional subspaces. Of particular

interest are the *marginalized* distributions of each parameter, obtained by integrating over the distribution of the other  $\mathcal{N} - 1$  parameters.

The above algorithms implement the following steps. (i) Let  $\zeta_1$  be a point-model in the parameter space. The spectra  $C_l$  of such model are computed and their corresponding likelihood  $\mathcal{L}_1$  is evaluated according to

$$-\ln \mathcal{L} = \sum_l \left( l + \frac{1}{2} \right) \left[ \frac{{}_dC_l|_0 B_l|^2 + N_l}{C_l|_0 B_l|^2 + N_l} + \ln \left( \frac{C_l|_0 B_l|^2 + N_l}{{}_dC_l|_0 B_l|^2 + N_l} \right) - 1 \right] + \text{const.} , \quad (8)$$

where  ${}_dC_l$  stands for either fiducial or realized spectra. The above expression holds for a single  $TT$  or  $EE$  spectrum; for its generalization to 3 spectra and a discussion of the effects of anisotropic noise, sky cuts, etc. see, e.g. Percival & Brown (2006). (ii) The algorithm then randomly selects a different point  $\zeta_2$ , in parameter space, according to a suitable *selection function*. The probability of accepting  $\zeta_2$  is given by  $\min(\mathcal{L}_2/\mathcal{L}_1, 1)$ . If  $\zeta_2$  is accepted, it is added to the chain, otherwise the multiplicity  $N_1$  of  $\zeta_1$  increases by 1. (iii) The whole procedure is then iterated starting either from  $\zeta_2$  or from  $\zeta_1$  again, until a stopping condition is met. The resulting chain is defined by  $(N_i \zeta_i)$ , where  $\zeta_i$  are the points explored and the multiplicity  $N_i$  is the number of times  $\zeta_i$  was kept.

The whole cycle is repeated until the chains reach a satisfactory *mixing* and a good *convergence*. The first requisite essentially amounts to efficiently exploring the parameter space, by quickly moving through its whole volume. In particular, the fact that the algorithm sometimes accepts points with lower likelihood than the current point, avoids permanence in local minima, while a careful choice of parametrization and of the selection function minimize the time spent exploring degenerate directions. A good convergence instead guarantees that the statistical properties of the chains (or of a suitably defined subset of the chains), correspond to those of the underlying distribution. Here we implement the convergence criterion of Gelman & Rubin (1992), based on  $R$ -ratio computation: convergence and mixing are reached when  $R - 1 \ll 0.1$ . Fulfilling such criterion requires  $N \sim 10^5$  points, in the cases considered here.

The algorithm was preliminarily tested by using  $\Lambda$ CDM as true cosmology and the set of parameter values shown in Figure 1. Such Figure reports the likelihood distributions found in this case, both for input parameters (with asterisk) and for several derived parameters as well. Besides confirming that input values are suitably recovered, mostly with fairly small errors, Fig. 1 shows a broad non-Gaussian distribution for  $w$  values, with little skewness but significant kurtosis. This is a well-known consequence of the geometrical degeneracy present in CMB spectra, and clearly shows the difficulty of CMB data to yield results on DE nature. The non-Gaussian behavior is even more accentuated for some derived parameter, as  $\Omega_{o,c}$ ,  $H_o$  and the Universe age  $\tau_o$ . We shall recover analogous features in the next plots; here we

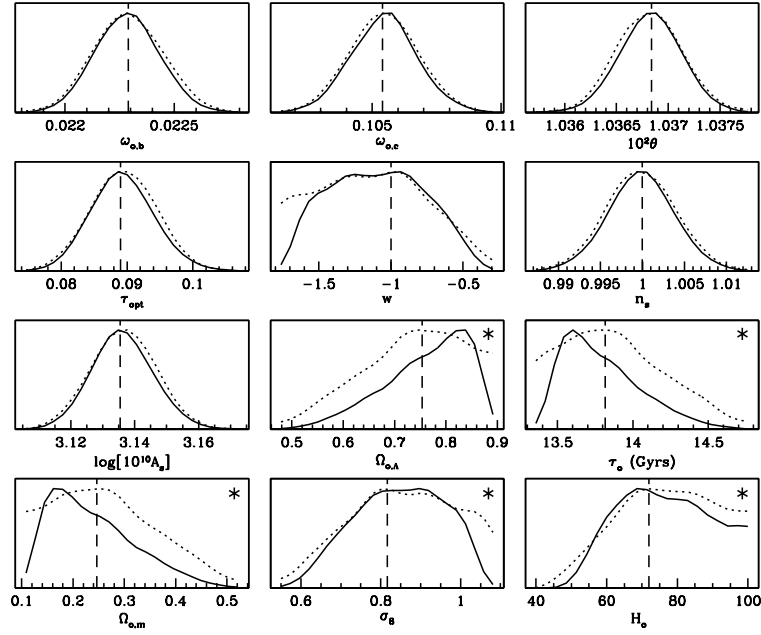


Fig. 1.— Marginalized *a posteriori* likelihood distributions (solid lines), when artificial data derive from a  $\Lambda$ CDM cosmology. Vertical lines yield the input parameter values. Derived parameter panels are marked by an asterisk. Dotted lines show the average likelihood distributions.



want to stress that they do not derive from fitting a partially unsuitable parameter set.

Figure 1 also shows how errors increase when passing to some secondary parameter, from primary parameters specifically devised to break degeneracies. For instance, the errors on  $\theta$  and  $\omega_{o,c}$  are  $\sim 0.03\%$  and  $\sim 1.3\%$ , respectively. From these parameters,  $H_o$  and  $\Omega_{o,c}$  are derived, whose errors are  $\sim 15\%$ .

The point here is that the primary variable is

$$\theta \equiv r_s(a^*)/D(a^*) , \quad (9)$$

$a^*$  setting the peak of the *quasi*-Gaussian last scattering band (LSB). It is then easy to see that

$$\begin{aligned} r_s(a^*) &= \frac{c}{H_o \Omega_{o,m}^{1/2}} \int^{a^*} \frac{da}{a^2} \frac{c_s(a)}{c} \frac{H_o \Omega_{o,m}^{1/2}}{H(a)} , \\ D(a^*) &= \frac{c}{H_o \Omega_{o,m}^{1/2}} \int_{a^*}^{a_o} \frac{da}{a^2} \frac{H_o \Omega_{o,m}^{1/2}}{H(a)} , \end{aligned} \quad (10)$$

so that  $\theta$  is apparently independent from  $H_o$  and  $\Omega_{o,m}$  as, in the former equation

$$\frac{H^2(a)}{H_o^2 \Omega_{o,m}} = \left(1 + \frac{a_{eq}}{a}\right) \left(\frac{a_o}{a}\right)^3 , \quad (11)$$

while, in the latter one

$$\frac{H^2(a)}{H_o^2 \Omega_{o,m}} = \left(\frac{a_o}{a}\right)^3 + (\Omega_{o,m}^{-1} - 1) g\left(\frac{a_o}{a}\right) , \quad (12)$$

and  $\Omega_{o,m}$  only sets the normalization of the latter term at the r.h.s., so that  $g(1) = 1$ . As a matter of fact, these equations exhibit a mild dependence of  $\theta$  on  $\omega_{o,m}$  and  $\omega_{o,b}$ , as  $a_o/a_{eq} = 2.41 \times 10^4 \omega_{o,m} (T_o/2.726 \text{ K})^{-4} [1.681/(1+0.227 N_\nu)]$  and  $(c_s/c)^{-2} = 3[1+(3/4)(\omega_{o,b}/\omega_{o,m})(a/a_{eq})(1+0.227 N_\nu)]$  (here  $T_o$  is the present CMB temperature and  $N_\nu$  is number of neutrino families in the radiative background). Information of  $\Omega_{o,m}$  and, thence, on  $H_o$  can be obtained only if the factor  $g(a_o/a)$ , yielding the evolution of the ratio between DE and matter at low redshift, is under control. It is certainly so if a  $\Lambda$ CDM model is assumed; but, if we keep  $w$  as free parameter, the uncertainty on it, ranging around 60%, reflect the difficulty to obtain the secondary parameters  $\Omega_{o,m}$  and  $H_o$ .

More in general, eq. (12) shows that CMB data are sensitive to a change of  $g(a_o/a)$  causing a variation of LSB distance  $D^*$ . On the contrary,  $\theta$  does not discriminate between different  $w(a)$  yielding the same  $D^*$ .

Incidentally, all that confirms that it is unnecessary to fix  $a^*$  with high precision, or to discuss whether it is a suitable indicator of the LSB depth. Knowing  $a^*$  with  $\sim 1\%$  approximation is quite suitable to this analysis.

#### 4. Dynamical DE vs. $w = \text{const.}$

Let us now discuss what happens if DE state equation, in the “real” cosmology, cannot be safely approximated by a constant  $w$ . To build data, we use then a SUGRA cosmology and our own extension of CAMB, directly dealing with a SUGRA potential both in the absence and in the presence of DM–DE coupling. Artificial data worked out for Model A with  $\beta = 0$  were then fit to the same parameters as in Figure 1. The whole findings are described in Table 2 (second column).

In Figure 2 we add further information, comparing the value distributions in fits assuming either a cosmology with  $w = \text{const.}$  or a SUGRA cosmology, then including  $\Lambda$ , as parameter, instead of  $w$ . The two fits agree well within  $1\text{-}\sigma$ , among themselves and with input values. In the Figure we show the fiducial case.

Let us briefly comment the results in the absence of coupling, when the fitting parameter set includes  $w$  instead of  $\Lambda$ : (i)  $\omega_{o,b}$  and  $\omega_{o,c}$  are recovered without any bias. (ii) The same holds for  $\theta$ , if a numerically refined value of  $a^*$  is used; the expression of  $a^*$ , as above outlined, has a precision  $\sim 1\%$ . Errors on  $a^*$ , however, are negligible in comparison with errors arising from the scarce knowledge of  $w(a)$ .

As outlined in the previous Section, the main problem to fix  $\Omega_{o,m}$ ,  $\Omega_{o,\Lambda}$ , and  $H_o$ , resides in the difficulty to determine the state equation of the expansion source since DE becomes substantially sub-dominant or dominant. This also makes clear why the formal error in the determination of the above three parameters is wider when the fit assumes a constant  $w$ : varying  $w$  yields an immediate and strong effect on DE contributions and state equation, extending up to now; on the contrary, only huge displacements of the energy scale  $\Lambda$  cause significant variations to DE contributions and state equation within the family of SUGRA cosmologies. In other terms, when  $\Lambda$  varies, the part of the functional space that  $w(a)$  covers is not so wide.

Accordingly, the greater error bars on  $\Omega_{o,m}$ ,  $\Omega_{o,\Lambda}$ ,  $H_o$ , found when we use  $w$  as a parameter, do not arise because we fit data to a “wrong” cosmology, but because varying  $w$  leads to a more effective spanning of the functional space of  $w(a)$ .

As a matter of fact, the reliability of the fit must be measured by comparing the likelihood of the best-fit parameter sets. Likelihood values, given in the next Section, do not discriminate between the two fits. Otherwise, a direct insight into such reliability is obtained by looking at the width of the marginalized *a posteriori* likelihood distributions on primary parameter values. Figure 2 then confirms that such distributions, although slightly displaced, have similar width for all primary parameters.

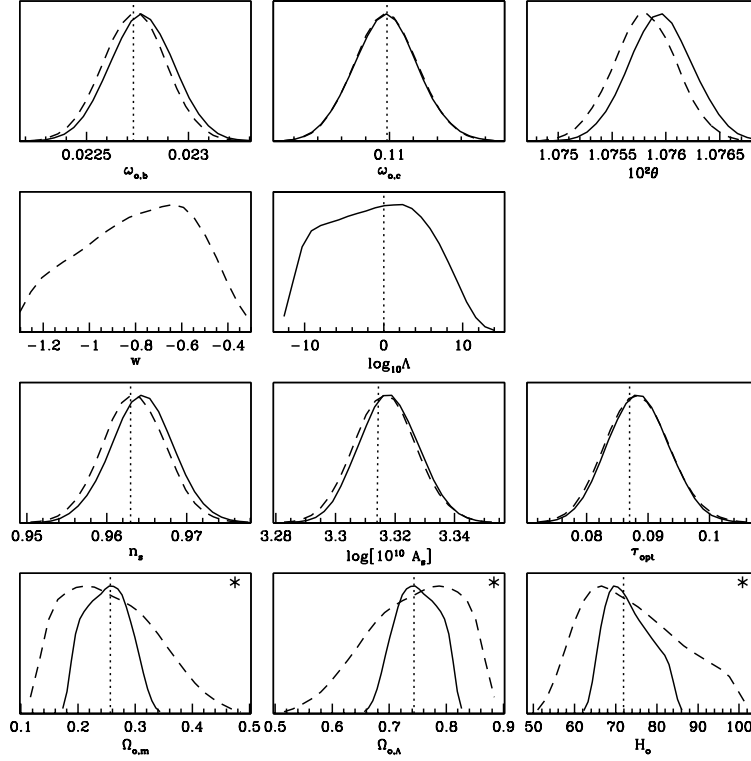


Fig. 2.— *Marginalized likelihood distributions on parameter values. Data built with an uncoupled SUGRA model. The parameter space for the fit includes either  $\log(\Lambda/\text{GeV})$  (solid lines) or a constant  $w$  (dashed lines). Vertical dotted lines show the input parameter values. Derived parameters plots are with asterisk.*

A general conclusion this discussion allows to draw is to beware from ever assuming that error estimates on secondary parameters, as  $\Omega_{o,m}$ ,  $\Omega_{o,b}$ , and  $H_o$ , are safe.

### 5. Coupled DE vs. $w = \text{const.}$

In cosmologies including cold DM and DE, the equation obeyed by the stress–energy tensors of the dark components

$$T^{(c)}{}^{\mu}{}_{\nu;\mu} + T^{(de)}{}^{\mu}{}_{\nu;\mu} = 0 , \quad (13)$$

yields

$$\frac{d}{d\tau}(\rho_c + \rho_{de}) = -3(\rho_c + p_c + \rho_{de} + p_{de})\frac{\dot{a}}{a} , \quad (14)$$

if their pressure and energy densities are  $p_c$ ,  $p_{de}$  and  $\rho_c$ ,  $\rho_{de}$ ;  $\tau$  is the conformal time and dots indicate differentiation in respect to  $\tau$ . Eqs. (13) and (14) state that no force, apart gravity, acts between standard model particles and the dark components. The eq. (13) is fulfilled if DM and DE separately satisfy the eqs.

$$T^{(de)}{}^{\mu}{}_{\nu;\mu} = CT^{(c)}\phi_{,\nu} , \quad T^{(c)}{}^{\mu}{}_{\nu;\mu} = -CT^{(de)}\phi_{,\nu} , \quad (15)$$

where  $T^{(de),(c)}$  are traces of the stress–energy tensors.  $C$  can be an arbitrary constant or, *e.g.*, a function of  $\phi$  itself; when  $C = 0$ , the two dark components are uncoupled and so are the cases we considered up to here.

It is however known (Wetterich 1995, Amendola 2000, Amendola & Quercellini 2003) that self consistent theories can be built with

$$C \equiv 4\sqrt{\frac{\pi}{3}}\frac{\beta}{m_p} \neq 0 , \quad (16)$$

so that  $\beta$  is used to parametrize the strength of DM–DE coupling.

By using MCMC techniques, we explored cosmologies with  $\beta = 0.05$  and  $0.1$  (Model A); we also report some results for  $\beta = 0.02$  (Model B). We aim to show that, when  $\beta$  is excluded from the parameter budget, the values MCMC provide for some parameters can be significantly biased, even though  $\beta$  is small.

In Table 2 (3rd–4th columns) we report the results of fitting the parameter set including constant  $w$ , in place of  $\Lambda$  and  $\beta$ . The Table allows an easy comparison with the uncoupled case, when all parameters unrelated to DE are nicely recovered. On the contrary, already for  $\beta = 0.05$ , the input  $\omega_{o,c}$  value is formally  $4.5 \sigma$ ’s away from best–fit, in the fiducial

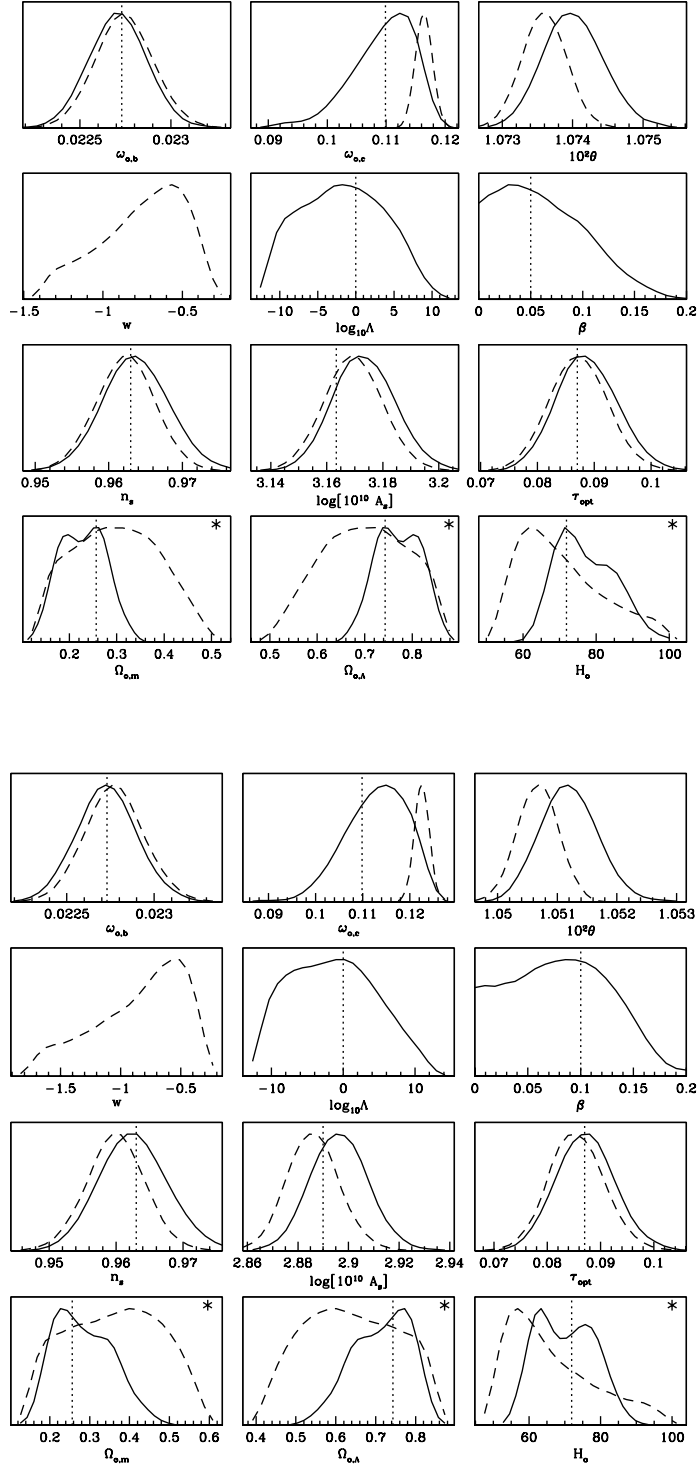


Fig. 3.— *Marginalized likelihood distributions on parameter values. Data built with coupled SUGRA models with  $\beta = 0.05$ ,  $\beta = 0.1$  (upper, lower panels). The parameter space for fits includes  $\log(\Lambda/\text{GeV})$  and  $\beta$  (solid lines) or just a constant  $w$  (dashed lines). Vertical dotted lines show the input parameter values. Pay attention to the different abscissa units in the two panel sets.*

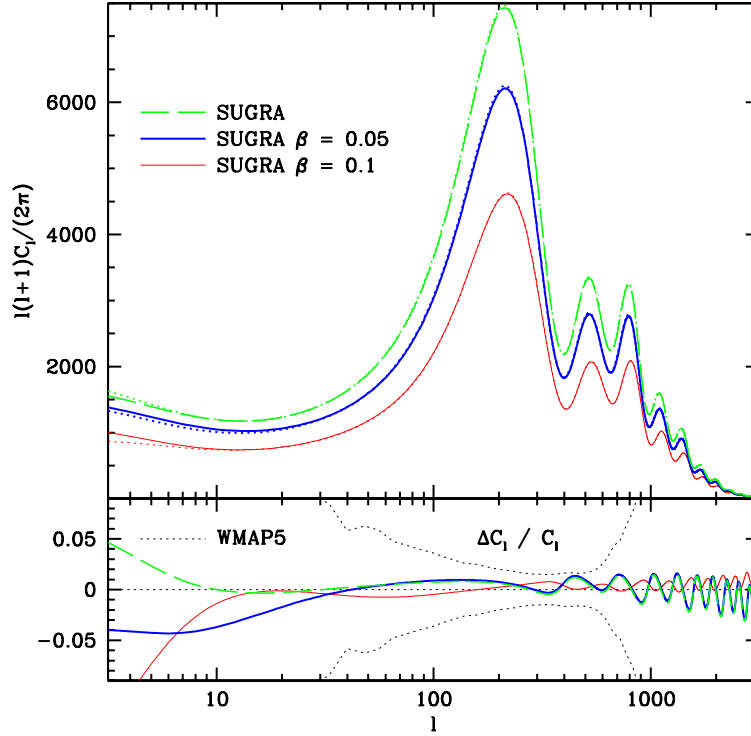


Fig. 4.— *Anisotropy spectra comparison.* The 3 values of  $\beta$  considered are clearly distinguished thanks to their different input normalization and to the line type indicated inside the upper frame. The dotted lines (hardly visible at low  $l$ 's in the upper panel) are the spectra of the corresponding best-fit model when assuming no coupling and  $w = \text{const.}$ . In the lower panel the relative differences between input and best-fit models are compared with WMAP5 error size.

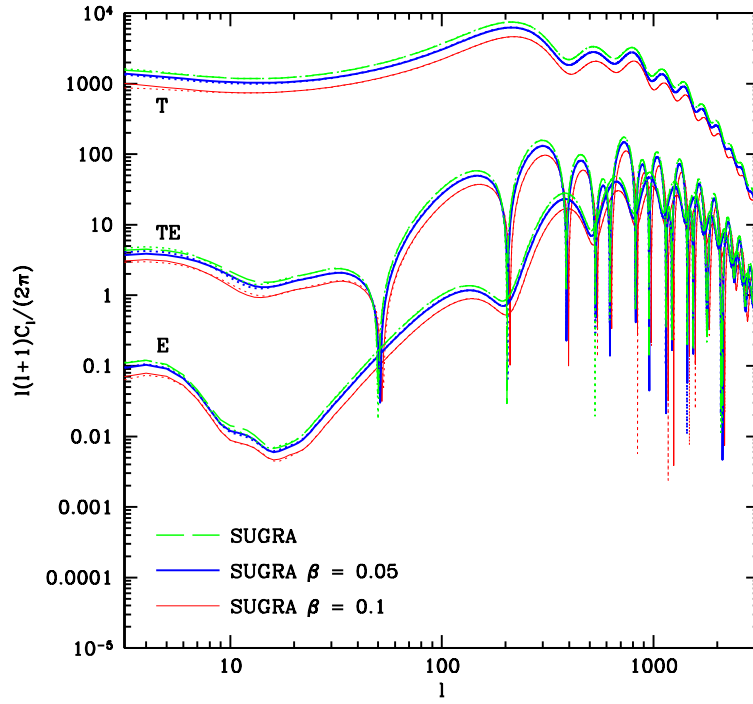


Fig. 5.— *The comparison made in the upper panel of the previous Figure is extended to ET and E-polarization spectra. Model differences are hardly visible at very low  $l$  and on the  $l$  values where the ET spectrum changes sign.*

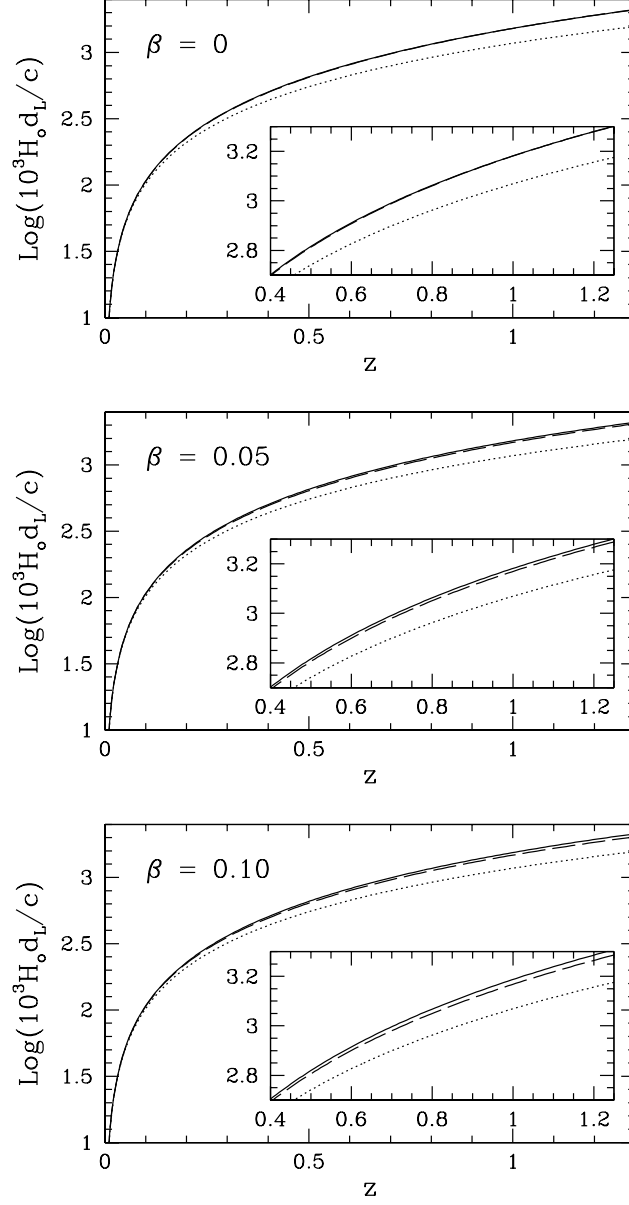


Fig. 6.— *Luminosity distance vs. redshift in models with  $\beta=0, 0.05, 0.10$  (solid lines). Each model is compared with the corresponding best-fit constant- $w$  model (dashed line) and with a SCDM model (dotted line) with equal  $\Omega_b$ .*



case, and more than 5  $\sigma$ 's in some realization. The effect is stronger for  $\beta = 0.1$ , yielding a discrepancy  $\sim 8 \sigma$ 's. That coupling affects the detection of  $\omega_{o,c}$  is not casual: in coupled models a continuous exchange of energy between DM and DE occurs.

Several parameters exhibit a non-Gaussian distribution, however. This is visible in Figure 3, where we also provide a comparison between likelihood distributions when (i) the fit includes just  $w$  or, instead, (ii) the parameter space includes  $\Lambda$  and  $\beta$ .

The comparison allows to appreciate that, in the (i) case,  $\omega_{o,c}$  is apparently much better determined than in the (ii) case. Appreciable discrepancies concern also the  $\theta$  parameter and they reflect onto the derived parameters  $\Omega_{o,b}$ ,  $\Omega_{o,m}$  and  $H_o$ , whose distribution however appears significantly non-Gaussian.

These results deserve to be accompanied by a comparison between the likelihood values in the different cosmologies. The following table shows  $\chi^2_{\text{eff}} \equiv -2 \ln(\mathcal{L})$  for the fiducial cases only:

	constant $w$	$\Lambda$ & $\beta$
	— — — — —	— — — — —
$\beta = 0$	0.175	0.887
$\beta = 0.05$	0.214	0.332
$\beta = 0.10$	0.778	0.251

The likelihood values for realizations are systematically smaller, as expected, but confirm the lack of significance shown here. Given that coupled models have 1 additional parameter over the  $w = \text{const}$  model, differences  $\Delta\chi^2_{\text{eff}} < \sim 1$  indicate that both models are an equally good fit of data. The conclusion is that spectral differences, between input and best-fit models, lay systematically below the error size. As a matter of fact, we are apparently meeting a case of degeneracy.

This statistical observation is corroborated by a direct insight into angular spectra, provided by Figures 4 and 5. We show the behaviors of the  $C_l$  spectra for the Model A, with  $\beta = 0$ ,  $\beta = 0.05$ ,  $\beta = 0.1$ , compared with the  $C_l$  for the best-fitting ( $w = \text{const.}$ ) model. Differences are so small to be hardly visible. Figure 4 refers just to anisotropy. In its lower panel the  $\Delta C_l / C_l$  ratio is compared with WMAP5 1- $\sigma$  error size ( $\Delta C_l$  is the difference between the spectra of the input and best-fit models). Notice that shifts by 1 or 2 units along the abscissa, at large  $l$  values, would still badly cut-off the apparent ratios. Clearly, degeneracy can be removed only if the error size is reduced by a factor  $\sim 10$  or more, in the region between the first deep and the second acoustic peak.

A further example we wish to add concerns a still smaller coupling intensity,  $\beta = 0.02$  (Model B, Table 3). At this coupling level, the MCMC meet all input parameter values within a couple of  $\sigma$ 's. A closer inspection of plots similar to Figure 3, not reported here,

shows that the probability of realizations yielding  $\omega_{o,c}$  formally more than  $3\text{-}\sigma$ 's away from the true value, is still  $> 8\%$ : the genie is still not completely back inside the lamp.

## 6. Other observables

The degeneracy observed in CMB spectra could be broken off through different observables. We plan to deepen this aspect in a forthcoming work, by building detailed data sets accounting from the dependence on cosmology of the expansion rate and growth factor.

A first insight into the actual situations can be however gained through an inspection of Hubble diagrams and transfer functions.

In Figure 6 we show the redshift dependence of the luminosity distances for models with  $\beta = 0, 0.05, 0.1$  and compare them with the corresponding best-fit models with constant  $w$ , as well as with  $\Lambda$ CDM models with the same value of  $\Omega_b$ . These plots clearly indicate that a fit with SNIa data would hardly allow any discriminatory signal: discrepancies from constant- $w$  model increase with  $\beta$ ; but, even for the  $\beta = 0.10$  case, they hardly exceed  $\sim 10\%$  of the difference from  $\Lambda$ CDM.

In Figure 7 we then exhibit the transfer functions  $T(k)$  (multiplied by  $k^{1.5}$  to improve the visibility of details) for models A.

In the cases  $\beta = 0$  and  $\beta = 0.05$ , we notice slight displacements for the BAO system and the slope. The actual setting of BAO's is however subject to non-linear effects and residual theoretical uncertainties are wider than the shifts in the plots. The change of slope is also easily compensated by a shift of  $n_s$  by  $\sim 0.01$ , widely within expected observational errors. Notice then that the relative position of the input and best-fit functions is opposite in the two cases. Accordingly, in the intermediate case  $\beta = 0.033$ , not shown in the plot, the overlap is almost exact and the observed scale dependence of the growth factor, at low redshift, does not break the degeneracy at all.

The situation is different when  $\beta > 0.05$  is considered. For  $\beta = 0.1$ , the BAO displacement is indeed relevant; to compensate for the change of slope, we would then require a shift of  $n_s$  greater than  $0.1$ .

A numerical analysis can therefore determine at which value, probably intermediate between  $0.05$  and  $0.1$ , the CMB spectra degeneracy is broken.

## 7. Conclusions

The nature of the dark cosmic components is unclear. DE could be a self-interacting field, yielding a scale dependent state parameter  $w(a)$ . Which bias does then arise on cosmological parameter estimates, if performed by assuming  $w = \text{const.}$ ? This question regards also parameters which do not describe DE; their estimate could be biased because the *true* model is not directly explored. A first conclusion of this work is that such bias exists but, in the cases we treated, yields acceptable displacements, within  $1\text{--}\sigma$ .

Suppose however that future data allow to exclude  $n_s = 1$ , within  $3\text{--}\sigma$ 's, when we assume  $w = \text{const.}$ . Setting  $n_s < 1$  discriminates among inflationary potentials. It would be however legitimate to assess that, at that stage, such conclusions would still be premature.

Our analysis was then extended to the case of DM–DE coupling. The idea that DM and DE have related origins or arise from the same field has been widely pursued (see, *e.g.* Kamenshchik, Moschella & Pasquier 2001, Bento, Bertolami & Sen 2002, 2004; Mainini & Bonometto 2004; for a review, see Copeland, Sami & Tsujikawa 2006). Coupling causes DM–DE energy exchanges and this option was first explored in the attempt to ease the *coincidence* problem.

Unfortunately, when a DM–DE coupling, strong enough to this aim, is added to models, predictions disagree with data. This does not forbid, however, that the physics of the dark components includes a weaker coupling or that a stronger coupling is compensated by other features (see, *e.g.*, La Vacca et al. 2008).

In this work we pointed out that a significant degeneracy exists, so that we can find an excellent fit of CMB data for coupled DE cosmologies just by using constant- $w$  uncoupled cosmologies. The fit is so good that even likelihood estimates do not allow to distinguish between the “true” cosmology and the best-fit constant- $w$  model, at the present or foreseeable sensitivity levels. *Unfortunately, however, the values obtained for several parameters are then widely different from input ones.*

In fact, if we ignore the coupling degree of freedom, when data are analyzed, we can find biased values for some primary parameter as  $\omega_{o,c}$ , for which input values lay  $\sim 5\text{--}\sigma$ 's away from what is “detected”. Also  $\Omega_{o,m}$  and  $H_o$ , which are secondary parameters, are significantly biased. In particular, with a coupling as low as  $\beta = 0.05$ , we found model realisations yielding  $H_o$  estimate  $\sim 2\text{--}\sigma$ 's away from the input value. If we keep to the fiducial case, however, the probability to find  $H_o \geq$  its input value is 36.5 % for  $\beta = 0.05$  and 26.5 % for  $\beta = 0.1$ . This outlines the tendency to find smaller values than “true” ones.

As a matter of fact, however, because of the uncertainty induced by our ignorance on

DE state equation, the width of errors on secondary parameter significantly exceeds the width for primary ones, and a  $5\text{-}\sigma$  discrepancy is partially hidden by such ignorance. This agrees with the fact that data analysis shows a significant increase of errors on secondary parameters when the set of models inspected passes from  $\Lambda$ CDM to generic- $w$  cosmologies. For instance, in the very WMAP5 analysis, the error on  $H_0$  increases by a huge factor  $\sim 6$ , when one abandons the safety of  $\Lambda$ CDM to explore generic constant- $w$  models. A general warning is then that errors obtained assuming  $\Lambda$ CDM are to be taken with some reserve.

An important question is whether the bias persists when different observables, besides CMB, are used. A preliminary inspection shows that SNIa data would hardly provide any discrimination. On the contrary an analysis of fluctuation growth can be discriminatory if  $\beta > \sim 0.07\text{--}0.08$ .

An even more discriminatory signal could be found in the  $z$  dependence of the growth factor is suitably analyzed. Observational projects aiming at performing a tomography of weak lensing, like DUNE-EUCLID (see, *e.g.*, Refregier et al. 2006, 2008), therefore, can be expected to reduce this degeneracy case.

ACKNOWLEDGMENTS. LPLC is supported by NASA grant NNX07AH59G and JPL-Planck subcontract no. 1290790.

## REFERENCES

- Amendola L. (2000) PR D**62**, 043511.
- Amendola L. & Quercellini C. (2003) PR D**68**, 023514.
- Amendola L., Campos G.C. & Rosenfeld R. (2004) astro-ph/0410543.
- Amendola L., Quercellini C., Tocchini-Valentini D. & Pasqui A. (2003) ApJ Lett. **583**, 53.
- Brax P. & Martin J. (1999) PL B**468**, 40; (2001) PR D**62**, 10350.
- Brax P., Martin J. & Riazuelo A. (2000) PR D**61**, 103505.
- Bento M.C., Bertolami O. & Sen A.A. (2002) PR D**66**, 043506; (2004) PR D**70**, 107304.
- Copeland E.J., Sami M. & Tsujikawa S. (2006) Int.J.Mod.Phys. D**15**, 1753.
- Colombo L.P.L. & Gervasi M. (2007) JCAP **0610**, 001.
- Foley R.J. et al. (2007) astro-ph/0710.2338.
- Gelman A. & Rubin D.B. (1992) Stat.Sc. **7**, 457.
- Hu W. & Sugiyama N. (1995) PR D**51**, 2599.
- Kamenshchik A., Moschella U. & Pasquier V. (2001) PL B**511**, 265.
- Komatsu Y. et al (2008) arXiv:0803.0547v1 (astro-ph) and APJ Suppl (in press).
- La Vacca G. & Colombo L.P.L. (2007) JCAP **0804**, 007 (2008).
- La Vacca G., S.A. Bonometto & Colombo L.P.L., arXiv:0810.0127 (astro-ph) and New Astr. (submitted)
- Lewis A. & Bridle S. (2002) PR D**66**, 103511.
- Mainini R. & Bonometto S.A. (2007) JCAP **06**, 020.
- Mainini R. & Bonometto S.A. (2004) PR Lett. **93**, 121301.
- Mainini R., Colombo L.P.L. & Bonometto S.A. (2005) ApJ **632**, 691.
- Majerotto E., Sapone D. & Amendola L. (2006) astro-ph/0610806.
- Maccio’ A.V., Quercellini C., Mainini R., Amendola L. & Bonometto S.A. (2004) PR D**69**, 123516.

- Perlmutter S. et al. (1997) ApJ **483**, 565; (1998) Nature **391**, 51.
- Percival W.J. & Brown M.L. (2006) MNRAS **372**, 1104.
- Ratra B. & Peebles P.J.E. (1988) PR D**37**, 3406.
- Refregier et al. (2006) Procs. of SPIE symposium "Astronomical Telescopes and Instrumentation", Orlando, May 2006, astro-ph/0610062.
- Refregier et al. (2008) arXiv:0807.4036 and to appear on Procs. of SPIE symposium "Astronomical Telescopes and Instrumentation", Marseille, June 2006
- Riess et al. (1997) ApJ **114**, 722.
- Spergel D.N. et al. (2007) ApJ Suppl. **170**, 377.
- Wetterich C. (1988) Nuc.Phys. B**302**, 483; (1995) A&A **301**, 32.

Input model: <i>SUGRA</i> ( $\Lambda = 1 \text{ GeV}$ ) with			
Parameter & Input value	$\beta = 0$ Av. value $\pm \sigma$	$\beta = 0.05$ Av. value $\pm \sigma$	$\beta = 0.1$ Av. value $\pm \sigma$
$10^2 \omega_{o,b}$	$2.274 \pm 0.015$	$2.274 \pm 0.015$	$2.277 \pm 0.017$
2.273	$2.278 \pm 0.015$	$2.275 \pm 0.015$	$2.295 \pm 0.017$
	$2.278 \pm 0.015$	$2.261 \pm 0.015$	$2.287 \pm 0.017$
	$2.280 \pm 0.015$	$2.278 \pm 0.015$	$2.282 \pm 0.017$
$\omega_{o,c}$	$0.1099 \pm 0.0013$	$0.1164 \pm 0.0014$	$0.1225 \pm 0.0016$
0.1099	$0.1083 \pm 0.0013$	$0.1166 \pm 0.0012$	$0.1225 \pm 0.0016$
	$0.1086 \pm 0.0013$	$0.1171 \pm 0.0014$	$0.1216 \pm 0.0016$
	$0.1104 \pm 0.0013$	$0.1163 \pm 0.0014$	$0.1225 \pm 0.0015$
$10^2 \theta$	$1.0758 \pm 0.0003$	$1.0736 \pm 0.0003$	$1.0507 \pm 0.0003$
1.072	$1.0759 \pm 0.0003$	$1.0736 \pm 0.0003$	$1.0509 \pm 0.0003$
	$1.0760 \pm 0.0003$	$1.0737 \pm 0.0003$	$1.0507 \pm 0.0003$
	$1.0759 \pm 0.0003$	$1.0736 \pm 0.0003$	$1.0507 \pm 0.0003$
$\tau_{opt}$	$0.088 \pm 0.005$	$0.087 \pm 0.005$	$0.085 \pm 0.005$
0.087	$0.087 \pm 0.005$	$0.903 \pm 0.005$	$0.084 \pm 0.005$
	$0.089 \pm 0.005$	$0.083 \pm 0.005$	$0.087 \pm 0.005$
	$0.093 \pm 0.005$	$0.079 \pm 0.005$	$0.078 \pm 0.005$
$w$	$-0.79 - 0.12 + 0.49$	$-0.75 - 0.30 + 0.26$	$-0.85 - 0.43 + 0.38$
—	$-0.84 - 0.27 + 0.25$	$-0.76 - 0.30 + 0.26$	$-0.96 - 0.44 + 0.82$
	$-0.81 - 0.26 + 0.25$	$-0.79 - 0.29 + 0.26$	$-0.67 - 0.34 + 0.37$
	$-0.87 - 0.28 + 0.28$	$-0.54 - 0.15 + 0.16$	$-0.63 - 0.24 + 0.23$
$n_s$	$0.963 \pm 0.004$	$0.962 \pm 0.004$	$0.960 \pm 0.004$
0.963	$0.966 \pm 0.004$	$0.962 \pm 0.004$	$0.958 \pm 0.004$
	$0.968 \pm 0.004$	$0.962 \pm 0.004$	$0.963 \pm 0.004$
	$0.959 \pm 0.004$	$0.961 \pm 0.004$	$0.959 \pm 0.004$
$\ln(10^{10} A_s)$	$3.3168 \pm 0.0102$	$3.1695 \pm 0.0101$	$2.8860 \pm 0.0101$
3.3144 for $\beta = 0$	$3.3127 \pm 0.0094$	$3.1699 \pm 0.0106$	$2.8866 \pm 0.0099$
3.1634 for $\beta = 0.05$	$3.3144 \pm 0.0103$	$3.1565 \pm 0.0095$	$2.8885 \pm 0.0102$
2.8902 for $\beta = 0.10$	$3.3310 \pm 0.0097$	$3.1486 \pm 0.0105$	$2.8736 \pm 0.0111$
$100 h$	$74.7 - 7.2 + 25.3$	$70.6 - 11.3 + 12.8$	$66.3 - 11.7 + 13.8$
71.9	$77.3 - 12.4 + 13.7$	$71.0 - 11.4 + 12.6$	$70.2 - 20.3 + 14.6$
	$75.7 - 12.3 + 13.3$	$71.9 - 11.0 + 12.6$	$60.9 - 11.1 + 10.5$
	$78.4 - 13.6 + 13.9$	$61.6 - 6.1 + 6.0$	$59.5 - 5.7 + 5.6$
$\Omega_{o,m}$	$0.255 - 0.084 + 0.169$	$0.300 - 0.100 + 0.095$	$0.360 - 0.133 + 0.127$
0.257	$0.235 - 0.105 + 0.077$	$0.296 - 0.096 + 0.096$	$0.325 - 0.123 + 0.140$
	$0.245 - 0.079 + 0.077$	$0.289 - 0.093 + 0.088$	$0.422 - 0.138 + 0.121$
	$0.233 - 0.101 + 0.084$	$0.379 - 0.074 + 0.073$	$0.431 - 0.103 + 0.097$

Table 2: *Results of an MCMC analysis, seeking the parameters listed in the first column, on artificial CMB data built with the parameter values also listed in the first column, but using a SUGRA cosmology, whose  $\Lambda$  and  $\beta$  are shown in the header. For each parameter, the first line yields results for the fiducial case, the next 3 lines for model realizations.*

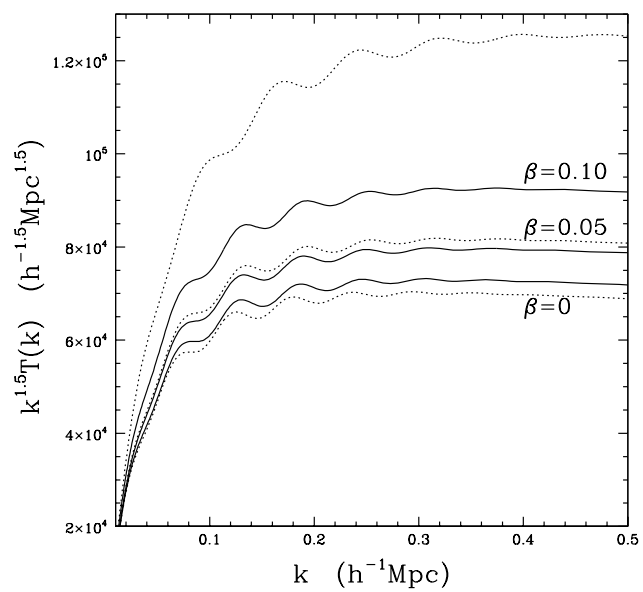


Fig. 7.— *Transfer functions for the models A. The dotted lines yield the transfer function of the models with  $w=\text{const.}$ , yielding the best-fit for CMB spectra.*



Input model: coupled <i>SUGRA</i> ( $\Lambda = 1 \text{ GeV}$ , $\beta = 0.02$ )	
Parameter & Input value	b.f. value $\pm \sigma$
$10^2 \omega_{o,b} = 2.400$	$2.400 \pm 0.016$
	$2.424 \pm 0.016$
	$2.423 \pm 0.017$
	$2.391 \pm 0.016$
$\omega_{o,c} = 0.1100$	$0.1127 \pm 0.0014$
	$0.1120 \pm 0.0013$
	$0.1121 \pm 0.0013$
	$0.1130 \pm 0.0014$
$10^2 \theta$	$1.11135 \pm 0.00032$
	$1.11174 \pm 0.00031$
	$1.11170 \pm 0.00032$
	$1.11108 \pm 0.00032$
$\tau = 0.1500$	$0.1515 \pm 0.0059$
	$0.1413 \pm 0.0067$
	$0.1412 \pm 0.0061$
	$0.1510 \pm 0.0061$
$w \text{ (at } z = 0)$	$-0.70 - 0.16 + 0.16$
	$-0.65 - 0.17 + 0.17$
	$-0.67 - 0.17 + 0.16$
	$-0.63 - 0.14 + 0.13$
$n_s = 1.0000$	$0.9998 \pm 0.0042$
	$0.9994 \pm 0.0039$
	$0.9990 \pm 0.0041$
	$0.9976 \pm 0.0041$
$\ln(10^{10} A_s) = 3.136$	$3.138 \pm 0.011$
	$3.119 \pm 0.013$
	$3.119 \pm 0.012$
	$3.139 \pm 0.012$
$100 h = 85$	$79 - 9 + 10$
	$77 - 10 + 10$
	$77 - 10 + 10$
	$75 - 8 + 8$
$\Omega_{o,m} = 0.185$	$0.254 - 0.057 + 0.058$
	$0.294 - 0.062 + 0.062$
	$0.268 - 0.059 + 0.059$
	$0.219 - 0.054 + 0.054$

Table 3: As previous Table, with different input values of cosmological parameters and  $\beta$  as small as 0.02